Nanoscale

Accepted Manuscript

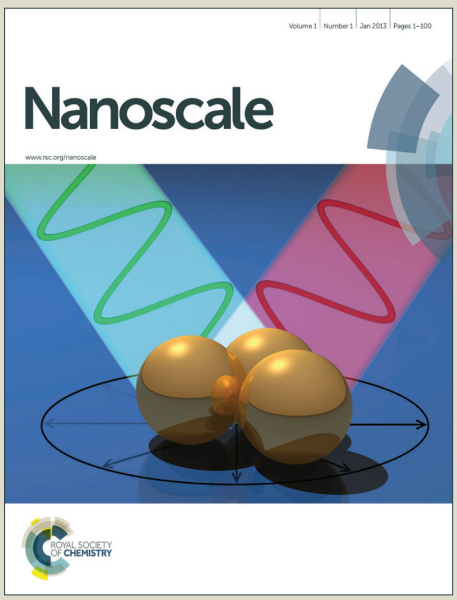

ROYAL SOCIETY OF CHEMISTRY

www.rsc.org/nanoscale

Theoretical Aspects of WS_2 Nanotube Chemical Unzipping

D. G. Kvashnin, [1,2*] L. Yu. Antipina, [3] P. B. Sorokin, [1,3,4] R. Tenne, [5] D. Golberg [6]

[1] National University of Science and Technology MISiS, 4 Leninskiy prospekt, Moscow, 119049, Russian Federation
[2] Emanuel Institute of Biochemical Physics of RAS, 119334 Moscow, Russian Federation
[3] Technological Institute of Superhard and Novel Carbon Materials, 7a Centralnaya Street, Troitsk, Moscow, 142190, Russian Federation
[4] Moscow Institute of Physics and Technology, 9 Institutsky lane, Dolgoprudny, 141700, Russian Federation
[5] Department of Materials and Interfaces, Weizmann Institute, Rehovot 76100, Israel
[6] World Premier International (WPI) Center for Materials Nanoarchitectonics (MANA), National Institute for Materials Science (NIMS), Namiki 1-1, Tsukuba, Ibaraki 3050044, Japan

Theoretical analysis of experimental data on unzipping multilayered WS_2 nanotubes by consequent intercalation of lithium atoms and 1-octanethiol molecules [C. Nethravathi et al. ACS Nano 7, 7311 (2013);] is presented. The radial expansion of the tube was described in the framework of continuum thin-walled cylinder approximation with parameters evaluated from *ab initio* calculations. Assuming that the driving force of attraction of the 1-octanethiol molecule is its reaction with the intercalated Li ions, *ab initio* calculation of 1-octanethiol molecule bonding with Li^+ was carried out. In addition, non-chemical interaction of 1-octanethiol dipole with an array of positive point charges peculiar to Li^+ was taken into account. Comparing between the energy gain from these interactions and the elastic strain energy of the nanotube allows us to evaluate a value of the tube walls deformation after 1-octanethiol molecules implantation. The *ab initio* molecular dynamics simulation confirmed our estimates and demonstrated that a strained WS_2 nanotube with decent concentration of 1-octanethiol molecules should indeed be unzipped into the WS_2 nanoribbon.

The establishment of a new field of two-dimensional nanostructures first comprising of freestanding graphene, [1] followed by boron nitride, [2] and transition metal dichalcogenide (TMD) [3] graphene-like nanosheets created clear possibilities for implementing many new nanomaterials in science, technology and industry. In contrast to the monolayers of graphene or *h*-BN, monolayers of MoS_2 and WS_2 consist of three-atom thick slab in which each metal atom is sandwiched between two layers of chalcogen atoms.

WS_2 and MoS_2 nanosheets have peculiar electronic properties (semiconducting band gap and high mobility of the carriers) which allow one to potentially apply these nanomaterials in the fields of nanoelectronics and nanophotonics. [3] The potentials for application of 2D TMDs in nanoelectronics can be further strengthened by their cutting into nanoribbons. This leads to a drastic change in the electronic, mechanical, and optical properties of these materials. There has been a number of theoretical papers showing that MoS_2 [4,5] and WS_2 [6] nanoribbons display semiconducting or metallic properties depending on their width and type of edges. Nowadays ultra-narrow MoS_2 and WS_2 nanoribbons can be fabricated inside and outside of carbon nanotubes. [5,6,7] Also MoS_2 nanorods and nanoflakes were fabricated. [8,9] However, until recently, there have been no reports in regards of fabrication of freestanding TMD nanoribbons.

It is well known that graphene nanoribbons could be fabricated through unzipping of carbon nanotubes by various methods. [10,11] TMDs can also form tubular structures similar to carbon nanotubes, [12] which can also be potentially unzipped into ribbons and nanoflakes, as has recently been shown for the case of WS_2. [13,14] The regarded work may establish a universal approach for nanotube unzipping and nanoribbon synthesis. Unpacking of the WS_2 nanotubes (WS_2NT) was caused by the lithiation and further intercalation by organic 1-octanethiol molecules followed by sonication. Therefore the underlining hypothesis of the current work was the following: the interaction between the 1-octanethiol molecules and lithium ions had led to the penetration of the 1-octanethiol molecules between the nanotube layers, especially between the outer layers, which caused the elastic expansion of the outer layers of the nanotube. Therefore, herein we focus on the theoretical verification of the process of WS_2NT unzipping. We based our work on the experimental fact that the unzipping of WS_2NT is caused by the intercalation of lithiated nanotube with organic molecules (1-octanethiol). We then address a hypothesis that penetration of the 1-octanethiol molecules between the nanotube walls leads to its radial expansion and further disruption followed by unzipping of the whole nanotube. The strain energy of the expanded tubes was calculated in continuum thin-walled cylinder approximation in the first part of the paper. Using the computed parameters of WS_2 lattice the dependence of deformation energy of the tubes upon the circumferential strain was then obtained. In the second part of the paper, we studied the intercalation of lithiated WS_2NT by reference organic molecules (1-octanethiol) and estimated the

energy gain of such process that can be consumed for expanding the layers and eventually unzipping the tube. The comparison of the energy gain with the elastic strain allows us to estimate the dependence of diameter of the WS_2NT upon the concentration of embedded 1-octanethiol molecules. The third part of the paper is devoted to the computational validation of the fact that, by densely packing organic molecules, a strained WS_2NT can be unzipped to a nanoribbon. In the final part, the electronic structures of initial WS_2NT and resulted WS_2 nanoribbon were discussed and compared with available theoretical and experimental data. [13]

Results and discussion

Figure 1a,b shows representative transmission electron microscopy (TEM) and high-resolution TEM (HRTEM) images of the starting WS_2 nanotubes. Figure 1c,d depicts the initial and final stages of the nanotube unzipping, as detailed in Ref. 13.

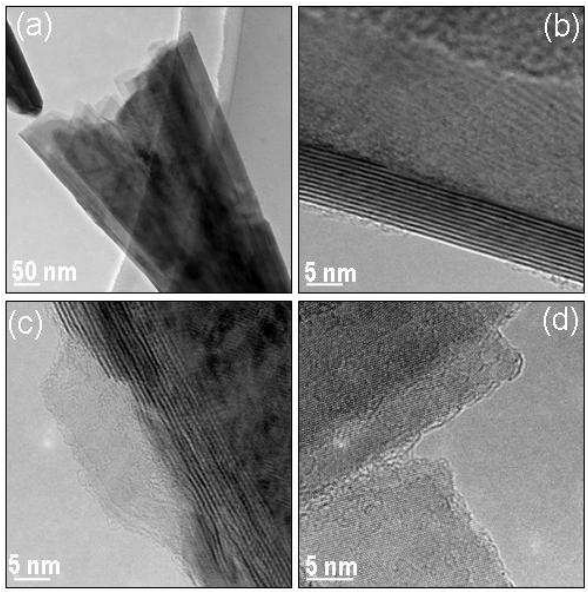

Figure 1 (a) Low-magnification TEM image of a WS_2 nanotube bundle; (b) high-resolution TEM image of a nanotube wall showing multi-layers; (c,d) HRTEM images of partially and fully unzipped nanotubes revealing atomically-resolved images of the WS_2 nanoribbons.

It is now important to theoretically understand and verify the process behind the unzipping of the WS_2NT; such description is the main point of the present work. The working hypothesis of the present study, as judged from the previously conducted experiments, is related to the elastic expansion of the intercalated tube. Subsequent sonication of the structure leads to the unzipping of already highly strained WS_2NT.

It was assumed that the continuum structure equivalent to WS_2NT is an isotropic thin-walled cylinder with a mean diameter of the corresponding nanotube. The elastic expansion of the tube causes the hoop stress σ_h which reduces the tube length and induces the longitudinal stress σ_L (radial stress is neglected). Therefore, we can describe the expression for the strain of the tube by Hook law as follows: [15,16]

$$\varepsilon_h = \frac{\sigma_h}{Y} - \frac{v\sigma_L}{Y} = \frac{PR}{2Yh}(2-v); \sigma_h = \frac{PR}{h}; \sigma_L = \frac{PR}{2h}, \quad (1)$$

where, ε_h is a hoop strain, Y and v are the in-plane Young's modulus and Poisson ratio of the continuum structure equivalent, respectively, P is the internal pressure which causes the expansion. Due to ambiguity in the single WS_2 layer thickness determination we used the in-plane stiffness $C = Y \cdot h = \frac{1}{A_0}\frac{\partial^2 U}{\partial \varepsilon^2}$ (where U is the strain energy computed per unit cell, A_0 is the equilibrium surface area of a WS_2 sheet and ε is the uniaxial strain). Therefore, the final expression for the strain energy U of the expanded continuum structure in terms of in-plane stiffness and hoop strain can be expressed in the following way:

$$U = \frac{2C\varepsilon_h^2}{2-\nu} \cdot S = \frac{2C\varepsilon_h^2}{2-\nu} \cdot 2\pi Rl\,, \qquad (2)$$

where S is the area of a WS_2 nanotube unit cell, l is the cell parameter in axial direction and R is the radius of the tube. Values of in-plane stiffness and Poisson ratio can be obtained directly from the *ab initio* calculations which were defined as 237.04 *N/m* and 0.3, respectively.

In Figure 2 comparison between the *ab initio* calculations and isotropic cylindrical tube approximation is shown for the case of a (9,9) WS_2 nanotube (the similar results were obtained for the tubes with other diameters and chirality). The close correspondence between the two data sets validates the chosen continuum model. This data is used for the evaluation of the strain within the elastically deformed WS_2 nanotubes intercalated by lithium ions and 1-octanethiol molecules.

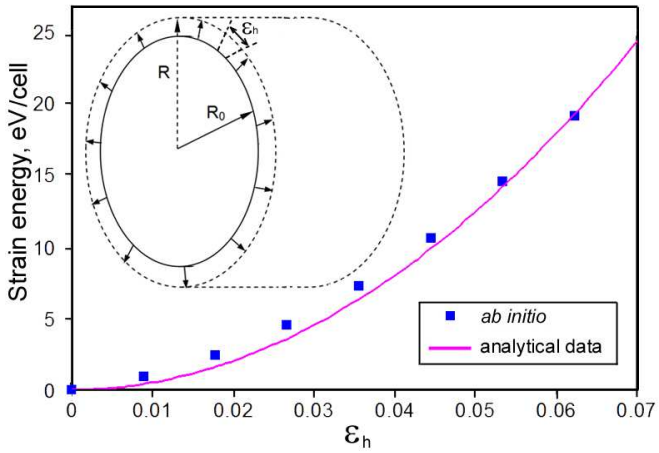

Figure 2 Strain energy of a (9,9) WS_2 nanotube as a function of the hoop strain for analytical data (solid curve) and *ab initio* calculations (points). The insets illustrate a schematic representation of the initial and the strained nanotube.

In the next step, we considered the mechanism of penetration of 1-octanethiol molecules between WS_2NT walls based on the assumption that the driving force of attraction of 1-octanethiol molecule is its interaction with the intercalated Li ions. *Ab initio* calculations show that 1-octanethiol molecule binds to lithium atom with the energy gain of -0.29 eV. If instead of a neutral atom the charged ion Li^+ (due to the charge transfer to the nanotube walls) is considered, the energy gain rises to -1.35 eV.

In addition, non-chemical interactions between the large dipole of 1-octanethiol and an array of positive point charges representing Li^+ ions was taken into account. The calculations show that the 1-octanethiol molecule has a dipole moment of 2.9 D. It was assumed that each 1-octanethiol molecule interacts with all lithium ions arranged between the nanotube walls uniformly (Figure 3) with the exception of the first lithium ion located before the 1-octanethiol molecule (marked as the red ball in Figure 3). The contribution of this first Li^+ was already taken into account during the *ab initio* calculation of the chemical reaction energy. It was suggested that Li^+ ions are densely packed between the walls without chemically binding with each other. Indeed, the distance between the neighboring intercalated Li^+ is about 4 Å, which is larger than the crystalline Li-Li bond length (2.67 Å) and larger than the distance in the molecular ion Li_2^+ (3.14 Å).

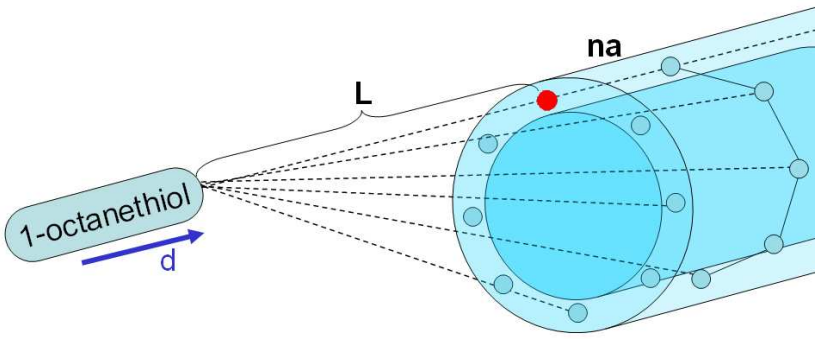

Figure 3 Schematic model of interaction between the dipole *d* of 1-octanethiol molecule and the set of a point charges representing the Li^+ ions. The closest Li ion to the 1-octanethiol molecule is marked in red.

The energy of the electrostatic interaction between the dipole and the set of point charges is defined as:

$$E_{dip} = qE \cdot \left|\bar{L} + n\bar{a}\right| = \frac{1}{4\pi\varepsilon\varepsilon_0} \cdot \frac{q \cdot d}{R^3} \cdot \left|\bar{L} + n\bar{a}\right| \cdot \sqrt{1 + 3\cos^2(\theta)},\ n = 0..\infty, \quad (1)$$

where d is an absolute value of a dipole moment of 1-octanethiol molecule, q is a charge of lithium ion, $R = \left|\bar{L} + n\bar{a}\right|$ is the distance between 1-octanethiol molecule and a given point charge; L is the distance between the dipole and the closest Li^+ from the first ring of a point charges (2.5 Å); θ is the angle between the dipole direction and the point charge; ε is a relative permittivity of 1-octanethiol solvent (where WS_2 nanotubes were unzipped in the original experiment [13]) which equals to 3.896 F/m. [17] Based on these estimates we can conclude that the value of released energy during the interaction between the dipole (1-octanethiol molecule) and the set of point charges equals to 0.19 eV and the total energy gain from the interaction of 1-octanethiol molecule with lithium ions arrives at 1.35 + 0.19 = 1.54 eV per 1-octanethiol molecule.

Assuming that all the gained energy is used for the radial expansion of the tube, the comparison between strain energy due to expansion and released energy due to the interaction of 1-octanethiol with Li^+ ions allows us to obtain a diagram of strain energy depending on the hoop strain of the tubes of different radii, see Figure 4. This diagram offers a visual estimation of the degree of nanotube stretching at a given concentration of the penetrated molecules.

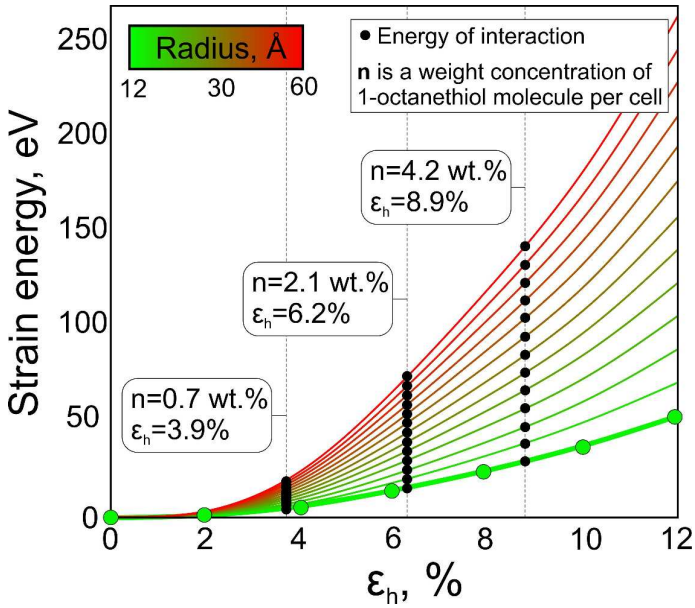

Figure 4 Dependence of the calculated strain energy upon the hoop strain ε_h for WS_2 nanotubes of different radii (from 12 to 60 Å). The black dots are the values of the total energy of interaction between the 1-octanethiol molecule and lithium ions at various 1-octanethiol weight

concentrations n which intercalation causes the nanotube expansion with corresponding hoop strain ε_h. The radius of unstretched WS_2 nanotube is marked by color gradient (from green, R = 12 Å to red, R = 60 Å). The resuls of DFT calculation for WS_2 nanotube (16,16) (R = 12 Å) are depicted by green circles

From Figure 4 it can be concluded that the released energy from the reaction between the 1-octanethiol molecules and lithium ions with maximum possible concentration (every $C_8H_{18}S$ molecule is paired with every Li^+ ion and occupied five WS_2 unit cells, n = 4.2 wt.%) is high enough to stretch the WS_2 nanotube up to 8.9 %. We subsequently carried out an *ab initio* molecular dynamics (MD) simulation to understand if this concentration is sufficiently large for the unzipping of the nanotube wall. Due to the limited computational resources, it is possible to simulate only a small double-walled nanotube (9,9)@(16,16). Moreover, due to the same limitation, it is not possible to use 1-octanethiol molecules in such simulation, therefore CH_4 molecules with nearly the same molecular lateral size were considered. The concentration of CH_4 molecules was taken as 9 molecules per unit cell which corresponds to n = 2.1 wt.%, as depicted in Figure 4. The relaxation of the nanotube with intercalated CH_4 molecules leads to the expansion of the tube to 7.6 % which corresponds to the obtained analytical data (6.2 %) and verifies our estimations.

The molecular dynamics simulation was carried out with a time step 1 fs, and the total simulation period was 10 ns. The most significant stages along the MD simulation period are shown in Figure 5 together with the corresponding energy profile of the system. The temperature of simulation was taken as 1000 K because it is not possible to simulate the long relaxation process at ambient temperatures. The double-walled nanotube without intercalated Li ions and CH_4 molecules is stable whereas the results of the MD evolution show (Figure **5**) that the intercalated structure was unzipped and a zigzag WS_2 nanoribbon with index 12 (according to the classification of graphene nanoribbons, 12ZWS_2NR) was formed. To validate such mechanism of nanotube unzipping, in addition, metadynamics simulation at 300 K of the same (9,9)@(16,16) WS_2NT was carried out. The simulation showed that the unzipping process had taken place after 800 metasteps passed at 300 K. This fact allows us to conclude on the correctness of the mechanism leading to WS_2 nanotube unzipping.

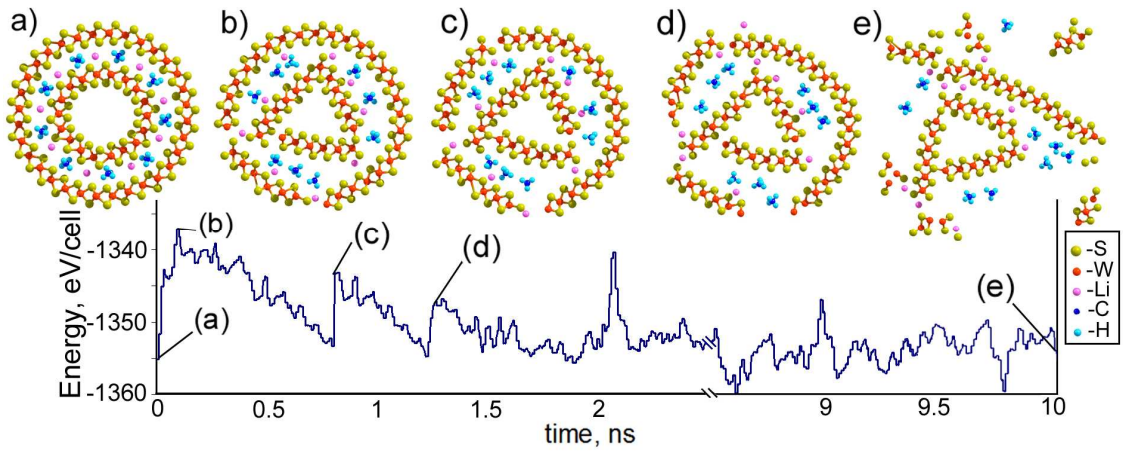

Figure 5 Potential energy and structural changes of a (9,9)@(16,16) intercalated WS_2 nanotube in MD simulations at T = 1000 K during a 10 ns period. The insets show the crucial moments in the structure evolution: a) the initial structure of (9,9)@(16,16) WS_2 nanotube with intercalated lithium atoms and methane molecules; b) first detachment of the part of the outer nanotube wall; c) detachment of the next part of the nanotube wall; d) partial deformation of the inner nanotube wall e) a finally unzipped structure of obtained from the (9,9)@(16,16) nanotube with resulting zigzag nanoribbon 12ZWS_2NR.

We also investigated the electronic properties of an initial double-walled WS_2 nanotube (9,9)@(16,16), a single-walled WS_2 nanotube (16,16) and the nanoribbon obtained from the unzipping of the former nanotube. In Figure 6 the band structures of the considered objects are presented. As one can see, both double- and single-walled WS_2 nanotubes display semiconducting properties with indirect band gaps of 0.9 eV and 1.55 eV, respectively while the formed nanoribbon displays a metallic character. This finding is in good agreement with the early published papers [6] and the latest work [13] which is in the prime focus of the present study.

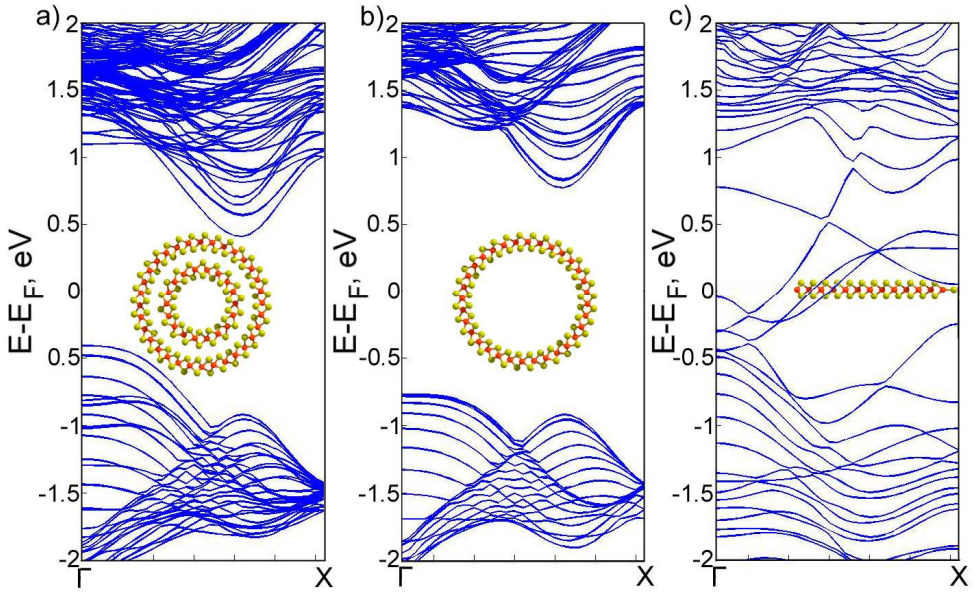

Figure 6 Band structure of a) (9,9)@(16,16) WS_2NT; b) (16,16) WS_2NT and c) 12ZWS_2NR. The Fermi level energy is taken as zero.

Conclusion

A simple model describing the latest experimental data of the unzipping process of WS_2 nanotubes [13] is presented. Based on the experimental fact that the effect of unzipping is caused by the intercalation of lithiated multi-walled WS_2NT by 1-octanethiol molecules, the hypothesis that the main reason for unzipping is the expansion of nanotube walls is proposed. The salient features of the mechanism of penetration of the molecules between the nanotube walls are presented. It is found that the approaching and binding of the 1-octanethiol molecules with the nanotube-intercalated Li^+ ions, is energetically favourable. The mechanical deformation of the nanotube walls is described in the framework of continuum thin-walled cylinder approximation with parameters evaluated from *ab initio* calculations. It is shown that using values of the in-plane stiffness (C) of 237.04 N/m and Poisson ration (v) of 0.3 provides an excellent correspondence between the analytical and the DFT-calculated data. Comparing the energy gain due to the interaction of 1-octanethiol molecule with Li^+ and the energy loss due to the elastic expansion of the wall, it is found that the penetration of 1-octanethiol between the nanotube walls can stretch a WS_2 nanotube up to 8.9 % at 4.2 wt.% concentration of the 1-octanethiol molecules. In order to understand if this strain is sufficiently large to lead to the nanotube wall unzipping, molecular dynamic simulation at 1000 K and metadynamics simulation at 300 K of a small double-walled (9,9)@(16,16) WS_2 nanotube system were carried out (in the simulation a smaller concentration corresponding to 2.1 wt.% of 1-octanethiol molecules was used). It is demonstrated that even under such circumstances the (9,9)@(16,16) WS_2 nanotube unzips and forms a WS_2 nanoribbon with index 12 (12ZWS_2NR). The investigated nanoobjects display different type of conductivity. It was finally concluded that the process of unzipping allows fabricating metallic planar WS_2 nanoribbons from the semiconducting tubes. The present results support recent experimental data and can pave the way toward the fabrication of transition metal dichalcogenides nanostructures with various electronic properties.

Methods

Computational details

Our calculations were performed using density functional theory [18,19] within the generalized gradient approximation of the Perdew-Burke-Ernzerhof [20] parameterization with periodic boundary conditions using Vienna *Ab-initio* Simulation Package. [21-23] PAW along with a plane wave basis set with energy cutoff of 300 eV was used. To calculate atomic and electronic structures, the Brillouin zone was sampled according to the Monkhorst–Pack [24] scheme with a 8 and 32 k-points in periodical direction. To avoid spurious interactions between neighboring structures in a tetragonal supercell, a vacuum layer of 15 Å in all nonperiodic directions was included. Structural relaxation was performed until the forces acting on each atom became less than 0.05 eV/Å. Unit cell of investigated double-walled WS_2NT with intercalated lithium atoms and methane molecules include up to 300 atoms depending on the NT radius. The molecular dynamics simualtions were carried out at constant temperature using the Nosé–

Hoover thermostat. [25,26] Temperature was taken as 1000 K. The total time of simulation was 10 ns with the time step 1 fs. Atomic structure was written after every ionic step. Metadynamics calculaions were performed in conditions of an Andersen thermostat [27] at a constant temperature of 300 K. The idea of metadynamics is the introduction of a history-dependent potential term, which fills the minima in the free energy surface. In this way the system can not go back to previously visited states until it could cross the energy barriers and undergo phase transitions. [28] History-dependent potential was constructed as a sum of Gaussians centered along the trajectory of the collective variables. Updating of bias potential by addition of Gaussian functions was made after each ionic step. The height of a Gaussian hill was taken as 10^{-3} eV and the Gaussian width was taken as 10^{-3} in units of the collective variables.

Acknowledgement

This work was supported by the Ministry of Education and Science of the Russian Federation (Agreement No. 11.G34.31.0061) within the Mega-Grant Program for the leading scientists (D.G.). We are grateful to the 'Chebishev' and 'Lomonosov' supercomputers of Moscow State University and the Joint Supercomputer Center of the Russian Academy of Sciences for the possibility of using a cluster computer for our quantum-chemical calculations. P.B.S. and L.Yu.A. acknowledge the support by the Russian Ministry of Education and Science (Contract No. 16.552.11.7014) and the Russian Foundation for Basic Research (project no. 12-02-31261). D.G.K. also acknowledges the support from the Russian Ministry of Education and Science (No. 948 from 21 of November 2012). R.T. acknowledges the support of the EU- ERC INTIF 226639 and EU-ITN Project MoWSeS 317451 projects. The authors are grateful to A.G. Kvashnin, Drs. C. Nethravathu, N. Kawamoto and Prof. Y. Bando for useful discussions.

References

1 K. S. Novoselov, *Rev. Mod. Phys.,* 2011, 83, 837;
2 D. Golberg, Y. Bando, Y. Huang, T. Terao, M. Mitome, C. Tang and C. Zhi, *ACS Nano,* 2010, 4, 2979;
3 Q. H. Wang, K. Kalantar-Zadeh, A. Kis, J. N. Coleman and M. S. Strano, *Nature Nanotech.,* 2012, 7, 699;
4 Y. F. Li, Z. Zhou, S. B. Zhang and Z. F. Chen, *J. Am. Chem. Soc.,* 2008, 130, 16739;
5 Z. Wang, H. Li, Z. Liu, Z. Shi, J. Lu, K. Suenaga, S. K. Joung, T. Okazaki, Z. Gu and J. Zhou *et al.*, *J. Am. Chem. Soc.,* 2010, 132, 13840;
6 Z. Wang, K. Zhao, H. Li, Z. Liu, Z. Shi, J. Lu, K. Suenaga, S. Joung, T. Okazaki and Z. Jin *et al.*, *J. Mater. Chem.,* 2010, 21, 171;
7 Z. Liu, K. Suenaga, Z. Wang, Z. Shi, E. Okunishi and S. Iijima, *Nat. Commun.,* 2011, 2, 213;
8 B. Visic, R. Dominko, M. K. Gunde, N. Hauptman, S. D. Skapin and M. Remskar, *Nanoscale Res. Lett.,* 2011, 6, 593;
9 X. Zheng, L. Zhu, A. Yan, C. Bai and Y. Xie, *Ultrason Sonochem,* 2004, 11, 83;
10 J. K. Dustin and J. M. Tour, *Macromol. Chem. Phys.,* 2012, 213, 1033;
11 L. Ma, J. Wang and F. Ding, *Chemphyschem.,* 2013, 14, 47;
12 R. Tenne, L. Margulis, M. Genut and G. Hodes, *Nature,* 1992, 360, 444;
13 C. Nethravathi, A. A. Jeffery, M. Rajamathi, N. Kawamoto, R. Tenne, D. Golberg and Y. Bando, *ACS Nano,* 2013, 7, 7311;
14 C. L. Choi, J. Feng, Y. Li, J. Wu, A. Zak, R. Tenne and H. Dai, *Nano Research,* 2013, 6, 921;
15. Fenner, R. T. Mechanics of Solids. (Blackwell Sci Publ, Oxford, London, Edinburgh, Boston, Melbourne, 1989).
16. Gere, J. M. ; Timoshenko, S. P. Mechanics of Materials. (Boston PWS Pub Co, 1997).
17 V. K. Agarwal, A. K. Sharma and P. Kumar, *J. Chem. Eng. Data,* 1977, 22, 127;
18 Y. Q. Zhu, T. Sekine, Y. H. Li, W. X. Wang, M. W. Fay, H. Edwards, P. D. Brown, N. Fleischer and R. Tenne, *Advanced Materials,* 2005, 17, 1500;
19 <. H. 8. N. M. , , 2011,
20 J. P. Perdew, K. Burke and M. Ernzerhof, *Phys. Rev. Lett,* 1996, 77, 3865;
21 G. Kresse and J. Hafner, *Phys. Rev. B,* 1993, 47, 558;
22 A. Margolin, R. Rosentsveig, A. Albu-Yaron, R. Popovitz-Biroa and R. Tenne, *J. Mater. Chem.,* 2003, 14, 617;
23 Y. Q. Zhu, T. Sekine, K. S. Brigatti, S. Firth, R. Tenne, R. Rosentsveig, H. W. Kroto and D. R. M. Walton, *J. Am. Chem. Soc.,* 2003, 125, 1329;
24 H. L. Tsai, J. Heising, J. L. Schindler, C. R. Kannewurf and M. G. Kanatzidis, *Chem. Mater.,* 1997, 9, 879;
25 W. G. Hoover, *Phys. Rev. A,* 1985, 31, 1695;
26 S. Nosé, *J Chem Phys,* 1984, 81, 511;
27 H. C. Andersen, *J Chem Phys,* 1980, 72, 2384;
28 A. Laio and M. Parrinello, *Proc. Nat. Acad. Sci.,* 2002, 99, 12562;